Columnar Assembly of Cyclic β-Amino Acid Functionalized with Pyranose Rings

Futoshi Fujimura, Tatsuya Hirata, Tomoyuki Morita, and Shunsaku Kimura*

Department of Material Chemistry, Graduate School of Engineering, Kyoto University, Kyoto-Daigaku-Katsura, Nishikyo-ku, Kyoto 615-8510, Japan

Yoshiki Horikawa and Junji Sugiyama

Research Institute for Sustainable Humanosphere (RISH), Kyoto University, Uji, Kyoto 611-0011, Japan

Received April 28, 2006; Revised Manuscript Received May 29, 2006

A novel cyclic trimer and tetramer of protected β-glycamino acids were synthesized and investigated on conformation and assembly formation. A characteristic point of these cyclic β-glycamino acids is their better solubility than other cyclic β-amino acids due to the pyranose rings. Thus, the assembling process of the cyclic molecules could be examined by CD or NMR spectroscopy. FT-IR and NMR measurements and geometry optimization revealed a highly symmetric and planar conformation for each cyclic β-peptide with all-*trans* amide groups. The amide groups in the cyclic peptides took a vertical orientation against the cyclic skeleton to be suitably arranged for intermolecular hydrogen bonds, which should promote formation of molecular assembly in a columnar structure through molecular stacking. These cyclic β-peptides were successfully crystallized to yield rod-shaped molecular assemblies in nanometer sizes. Evidence for the columnar structure in the crystals was obtained by electron diffraction analysis, which showed a layer spacing of ca. 4.8 Å. Interestingly, the molecular assembly of the cyclic trimer showed a high aspect ratio, width less than 40 nm, and length more than 2 μm, suggesting stable molecular stacking in the column.

Introduction

Sugar amino acids (SAAs) are pyranoid or furanoid containing amino and carboxyl groups.[1−7] In recent decades, α-SAAs,[8] β-SAAs,[9−11] γ-SAAs,[12] δ-SAAs,[13−16] and alkylated-SAAs[17] have been investigated widely on synthesis, conformation, secondary structures of their homooligomers, and biological activities. Especially, cyclic SAAs attract much attention in terms of biological activities and host−guest chemistry on the basis of their pyranose or furanose rings.[18−24] Since cyclic SAAs belong to the category of cyclic peptides, which have been shown as useful building blocks for molecular assembly,[25] it is interesting to explore the ability of cyclic SAAs for the molecular architecture with biological activities or functions.

Cyclic β-peptides are known to form unique and interesting nanotube assemblies due to the molecular stacking by intermolecular hydrogen bonds.[26] We have reported that cyclic β-tripeptide with cyclohexyl rings at the side chains formed bundles of the nanotubes.[27] Interestingly, the molecular columns were arranged in a parallel way to enhance dipole moment of all the amide groups in the bundle. However, it is generally difficult to investigate on conformation of the component in the molecular assemblies (especially cyclic peptides) and to control the morphology of assemblies because of a severe solubility problem.[26,28] To overcome this problem, previous reports showed some strategies: (i) replacement with *N*-methyl-amide derivatives to inhibit hydrogen-bond formation,[29] (ii) introduction of hydrophilic side chains (such as NH_3^+ or CO_2^-),[30] and (iii) addition of Li^+ ions for shielding carbonyl groups from intermolecular interactions.[31] However, another way to improve the solubility problem is still required for applications of the nanotubes to wide aspects.

Under these backgrounds, we designed here novel cyclic β-peptides composed of β-SAAs and investigated their molecular assembling properties. β-SAA with a pyranose ring as the side chain is expected to improve solubility of its cyclic oligomers due to the multiple hydroxyl groups. Further, the pyranose ring has a merit for chemical modification to functionalize the exterior of the molecular assembly. Herein we describe synthesis, conformation, and assembly formation of novel cyclic homotrimer and homotetramer of β-glycamino acids, which are protected with acetyl groups on the hydroxyl groups (GA(OAc)) (Figure 1).

Experimental Section

Measurements. NMR spectra were recorded with a Bruker DPX-400 spectrometer. Fast-atom bombardment (FAB) mass spectra were obtained on a JEOL JMS HX-110A spectrometer using 2, 4-dinitrobenzyl alcohol as matrix. FT-IR measurements were performed by the KBr method with a Nicolet 6700 FT-IR spectrometer.

Optical and Dark Field Microscopy. Optical microscopy was performed using an Olympus IX70 with polarizing filters. Compound **1** was recrystallized slowly from 2,2,2-trifluoroethanol/ethanol (2/1 v/v) (ca. 1 mg/mL). The crystals were sandwiched between two glass slides and observed in the cross-nicol configuration with a sensitive tint plate positioned between the polarizers. Dark field microscopy was performed using an Olympus BX 51 equipped with a 100× oil immersion lens and mercury bulb UV illumination. For this measurement, **2** was recrystallized from pyridine/methanol (3/1 v/v) (ca. 1 mg/mL), and the crystals were sandwiched between two glass slides. Photomicrographs were taken using a camera directly mounted on these microscopes.

Transmission Electron Microscopy and Electron Diffraction. The images and diffractions were taken by using a JEOL JEM-2000EXII

* To whom correspondence should be addressed. Fax: +81-75-383-2401. Tel: +81-75-383-2400. E-mail: shun@scl.kyoto-u.ac.jp.

10.1021/bm060415y CCC: $33.50
Published on Web 07/13/2006

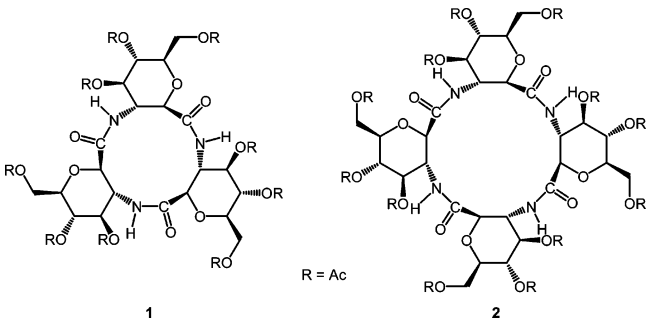

Figure 1. Chemical structures of cyclic timer **1** and tetramer **2** having pyranose rings.

(JEOL, Japan) at an accelerating voltage of 100 kV. For the observation along the column axis, the crystal of **1** or **2** was dispersed in 2,2,2-trifluoroethanol/ethanol (1/2 v/v) or pyridine/acetonitrile (1/4 v/v) (ca. 0.1 mg/mL). A drop of dispersed suspension was mounted on a carbon-coated Cu grid and stained negatively with 2% uranyl acetate containing 1% trehalose.

The electron diffraction diagrams were obtained in the microdiffraction mode.[32,33] A small condenser with an aperture of 20 μm was inserted in the second condenser lens, and the first condenser lens was fully overfocused to achieve an electron probe of approximately 100 nm at the sample level. The samples were observed at 2500× under extremely low-dose conditions, at the limit of the dark current, with the help of an image intensifier (Fiber Optics Coupled TV, Gatan). After proper zone identification, the beam was manually blanked. The beam intensity was then set to the desired value, and the electron microscope was switched to the diffraction mode. The beam was deblanked, followed immediately by the opening of the mechanical shutter and the recording of the diffraction diagram on a preset film. The sample to camera length was calibrated with the (111) diffraction ring of evaporated Au particles.

Theoretical Calculation of Molecular Energies. The molecular energies (internal energy) of **1** and **2** were calculated as follows. The initial geometry was generated by the CAChe software (Fujitsu Co., Ltd., Japan), and was optimized by a semiempirical Austin Model 1 (AM1) method in the MOPAC 2002 package.[34] Using the obtained geometry as input, ab initio calculation was carried out using Gaussian 03 program.[35] The geometry was further optimized at the Hartree−Fock (HF) level with frequency calculation for the zero-point energy. With the optimized geometry at the HF level, the single-point energy was calculated based on density functional theory with the Becke's three-parameter hybrid functional and Lee−Yang−Parr correlation (B3LYP) method. The 3-21G(d) basis set was used in both calculations. Finally, the internal energy of the molecule was obtained as the sum of the zero-point energy and single-point energy.

Synthesis. Linear Dimer (5). The Boc group of compound **4** (644 mg, 1.17 mmol) was deprotected by treatment with TFA (6.4 mL) and anisole (644 μL). Obtained trifluoroacetate salt was washed with diethyl ether and dried up in vacuo for 2 h. The salt and **4′** (560 mg, 1.29 mmol) were dissolved in DMF (3 mL), and DIEA (710 μL, 3.26 mmol) was added. The mixture was cooled to 0 °C and then HATU (590 mg, 1.55 mmol) was added. After being stirred at 0 °C for 3 h and at room temperature for 24 h, the mixture was concentrated, diluted with $CHCl_3$, and washed with 4% aqueous $KHSO_4$ (three times), 4% aqueous $NaHCO_3$ (three times), and saturated aqueous NaCl. The organic layer was dried over $MgSO_4$ and evaporated, and the residue was washed with diethyl ether to provide **5** (842 mg, 77%) as a white solid: R_f 0.40 (20:1 $CHCl_3$/MeOH). ^{1}H NMR (400 MHz, $CDCl_3$): δ 7.90, 7.61, 7.49 (d, t, t, 5H, phenyl), 6.83 (d, 1H, amide), 5.50 (t, 1H), 5.45−5.36 (dd, 2H, CO_2CH_2CO), 5.32 (t, 1H), 5.18−4.99 (m, 3H), 4.68 (d, 1H), 4.45 (d, 1H), 4.28−4.04 (m, 5H), 3.87 (d, 1H), 3.79−3.67 (m, 2H), 3.60−3.50 (m, 1H), 2.09−1.93 (m, 18H, acetyl), 1.36 (s, 9H, Boc). FAB-MS (matrix: nitrobenzyl alcohol) (*m*/*z*): calcd for $C_{39}H_{51}N_2O_{20}$ [(M + H)$^+$], 866.30; obsd, 867.35.

Linear Trimer (6). The Boc group of dimer **5** (364 mg, 0.41 mmol) was deprotected by treatment with TFA (3.6 mL)/anisole (364 μL). Obtained trifluoroacetate salt was washed with diethyl ether and dried up in vacuo for 2 h. The salt and **4′** (178 mg, 0.41 mmol) were dissolved in DMF (3 mL), and DIEA (235 μL, 1.35 mmol) was added. The mixture was cooled to 0 °C, and then HATU (187 mg, 0.49 mmol) was added. After being stirred at 0 °C for 3 h and at room temperature for 24 h, the mixture was concentrated, diluted with $CHCl_3$, and washed with 4% aqueous $KHSO_4$ (three times), 4% aqueous $NaHCO_3$ (three times), and saturated aqueous NaCl. The organic layer was dried over $MgSO_4$ and evaporated, and the residue was washed with diethyl ether to provide **6** (371 mg, 77%) as a white solid: R_f 0.54 (20:1 $CHCl_3$/MeOH). ^{1}H NMR (400 MHz, $CDCl_3$): δ 7.90, 7.61, 7.48 (d, t, t, 5H, phenyl), 7.46 (d, 1H, amide), 7.07 (d, 1H, amide), 5.77 (t, 1H), 5.49−5.38 (dd, 2H, CO_2CH_2CO), 5.35 (t, 1H), 5.14−5.02 (m, 4H), 4.77 (d, 1H, urethane), 4.42−3.93 (m, 7H), 3.98−3.90 (m, 2H), 3.83−3.56 (m, 6H), 2.08−1.93 (m, 27H, acetyl), 1.39 (s, 9H, Boc). FAB-MS (matrix: nitrobenzyl alcohol) (*m*/*z*): calcd for $C_{52}H_{67}N_3O_{28}Na$ [(M + Na)$^+$], 1204.38; obsd, 1204.43.

Cyclic Trimer (1). The pac group and the Boc group of compound **6** (214 mg, 0.20 mmol) was deprotected by zinc-catalyzed (10 mmol) hydrogenolysis and treatment with TFA (2.2 mL)/anisole (220 μL), respectively. Obtained trifluoroacetate salt was washed with diethyl ether and dried up in vacuo for 2 h. The salt was dissolved in DMF (20 mL), and a solution of BOP (133 mg, 0.30 mmol) in DMF (0.5 M) and a solution of HOAT (41 mg, 0.30 mmol) in DMF (0.5 M) were added. Then a solution of DIEA (210 μL, 1.20 mmol) in DMF (0.1 M) was added slowly (over 1 h via syringe pump). The reaction mixture was stirred at room temperature for 12 h. The mixture was concentrated, and the residue was washed with hot methanol (50 °C) several times, giving rise to acetylated cyclic compound **1** (132 mg, 70%) as a white solid. ^{1}H NMR (400 MHz, DMSO-d_6): δ 8.03 (d, 3H, J = 9.0 Hz, amide), 5.13 (dd, 3H, $J_{2,3}$ = 10.0 Hz, $J_{3,4}$ = 9.5 Hz, H-3), 4.79 (dd, 3H, $J_{4,5}$ = 9.5 Hz, H-4), 4.13−4.09 (m, 3H, H-2), 4.09−4.00 (dd, 6H, J = 12.6, 2.5 Hz, H-6), 3.87 (d, 3H, J = 10.5 Hz, H-1), 3.85−3.80 (m, 3H, H-5), 1.98, 1.96, 1.86 (s, 27H, acetyl). ^{13}C NMR (400 MHz, DMSO-d_6): δ 170.2, 170.1 (CH_3CO_2, C3, C4), 169.5 (CH_3CO_2, C6), 166.1 (amidecarbonyl), 77.2, 74.7, 73.7, 68.5, 62.5, 50.4 (C1, C3, C5, C4, C6, C2), 20.7, 20.6 (CH_3CO_2, C3, C4), 20.4 (CH_3CO_2, C6). IR (KBr): 3336, 3298, 2884, 1749, 1686, 1550, 1389, 1231, 1109, 1034 cm^{-1}. FAB-MS (matrix: nitrobenzyl alcohol) (*m*/*z*): calcd for $C_{39}H_{51}N_3O_{24}Na$ [(M + Na)$^+$], 968.27; obsd, 968.24.

Linear Tetramer (7). The Boc group of dimer **5** (300 mg, 0.346 mmol) was deprotected by treatment with 4 N HCl/1,4-dioxane (2.60 mL, 10.4 mmol). Obtained hydrochloride salt was washed with diethyl ether and dried up in vacuo for 2 h. The salt and the C-terminal free dimer (285 mg, 0.381 mmol) were dissolved in DMF (6 mL), and DIEA (156 μL, 0.894 mmol) was added. The mixture was cooled to 0 °C and then HATU (174 mg, 0.457 mmol) was added. After being stirred at 0 °C for 3 h and at room temperature for 24 h, the mixture was concentrated, diluted with $CHCl_3$, and washed with 4% aqueous $KHSO_4$ (three times), 4% aqueous $NaHCO_3$ (three times), and saturated aqueous NaCl. The organic layer was dried over $MgSO_4$ and evaporated, and the residue was purified by silica gel column chromatography (50:1 $CHCl_3$/ MeOH) to provide **7** (471 mg, 0.315 mmol, 81%) as a white solid: R_f 0.69 (10:1 $CHCl_3$/MeOH). ^{1}H NMR (400 MHz, $CDCl_3$): δ 7.92, 7.61, 7.49 (d, t, t, 5H, phenyl), 6.96 (m, 2H, amide), 5.57 (t, 1H), 5.50−5.42 (dd, 2H, CO_2CH_2CO), 5.40 (m, 1H), 5.14−4.99 (m, 6H), 4.46 (d, 1H), 4.31−4.12 (m, 8H), 4.05 (m, 2H), 3.97−3.86 (m, 4H), 3.74−3.63 (m, 6H), 2.10−1.93 (m, 36H, acetyl), 1.38 (s, 9H, Boc). FAB-MS (matrix: nitrobenzyl alcohol) (*m*/*z*): calcd for $C_{56}H_{84}N_4O_{36}$-Na [(M + Na)$^+$], 1519.47; obsd, 1519.47.

Cyclic Tetramer (2). The pac group and the Boc group of compound **7** (278 mg, 0.19 mmol) was deprotected by zinc-catalyzed (9.3 mmol) hydrogenolysis and treatment with TFA (2.8 mL)/anisole (280 μL), respectively. Obtained trifluoroacetate salt was washed with diethyl ether and dried up in vacuo for 2 h. The salt was dissolved in DMF

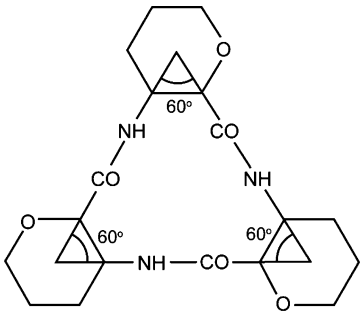

Figure 2. Schematic illustration of the bond angle between the amino group and the carboxyl group of β-amino acid in the cyclic trimer **1**.

(15.7 mL), and a solution of BOP (97 mg, 0.22 mmol) in DMF (0.5 M) and a solution of HOAT (30 mg, 0.30 mmol) in DMF (0.5 M) were added. Then a solution of DIEA (153 μL, 0.88 mmol) in DMF (0.1 M) was added slowly (over 1 h via syringe pump). The reaction mixture was stirred at room temperature for 12 h. The mixture was concentrated, and the residue was washed with hot methanol (50 °C) several times, giving rise to acetylated cyclic compound **2** (165 mg, 69%) as a white solid. ^{1}H NMR (400 MHz, pyridine-d_5): δ 10.62 (d, 4H, J = 8.0 Hz, amide), 5.93 (dd, 4H, H-3), 5.24 (dd, 4H, H-4), 4.92−4.89 (m, 4H, H-2), 4.09−4.00 (dd, 8H, H-6), 3.87 (d, 4H, J = 11.5 Hz, H-1), 3.76−3.73 (m, 4H, H-5), 2.12, 2.06, 1.96 (s, 36H, acetyl). ^{13}C NMR (400 MHz, pyridine-d_5): δ 170.6, 170.3 (CH_3CO_2, C3, C4), 169.8 (CH_3CO_2, C6), 168.3 (amidecarbonyl), 79.9, 77.0, 74.4, 69.3, 63.1, 52.3 (C1, C3, C5, C4, C6, C2), 20.8, 20.7 (CH_3CO_2, C3, C4), 20.5 (CH_3CO_2, C6). IR(KBr): 3336, 3298, 2884, 1749, 1686, 1550, 1389, 1231, 1109, 1034 cm^{-1}. FAB-MS (matrix: nitrobenzyl alcohol) (m/z): calcd for $C_{52}H_{68}N_4O_{32}Na$ [(M + Na)$^+$], 1283.37; obsd, 1283.40.

Results and Discussion

Peptide Design. We are interested in molecular assemblies with dipole moment, which may lead to functionalized materials.[36−38] Cyclic β-peptides are a prerequisite for obtaining nanotube assembly, especially with intrinsic dipole moment from the following reports: (i) cyclic peptides composed of β- or δ-amino acids may have essential dipole moment due to parallel orientation of amide bonds against the cyclic skeleton,[39] and (ii) the cyclic trimer of glucosyluronic acid methylamine, which is a family of cyclic δ-amino acids, no longer stuck up via intermolecular hydrogen bonds due to the flexible ring structure.[40] Further, taking the solubility problem of cyclic β-amino acids into consideration, β-SAA was chosen here for the component of cyclic peptides to build up tubular assemblies with dipole moment.

Cyclic tri- and tetra-β-peptides are known to have a rigid and planar structure with all-*trans* amide groups.[26,28,30,31,41] We therefore designed a novel cyclic trimer and tetramer having glucosamine units as shown in Figure 1. The dihedral angles of C$^\alpha$−C−N−C$^\beta$ (amide groups) in the cyclic trimer and tetramer generally take 180° (*trans*).[41,42] On the other hand, the dihedral angle H−N−C$^\beta$−H$^\beta$ in cyclic β-peptide having cyclohexyl rings at the side chains was found to be nearly 180° due to the favorable chair form of the six-membered ring structure.[27] When the cyclic trimer or tetramer is assumed to take the highly symmetrical conformation under these two preferences, their molecular geometry would be equilateral triangle (Figure 2) or square where the SAA units and peptide bonds would occupy the apexes of the triangle or the square and the sides, respectively. Since the bond angle between N−C$^\beta$ and C$^\alpha$−C(=O) will favorably be 60°, the cyclic trimer will be stably formed because the inner angle of equilateral triangle is 60°. However, for the square structure of the cyclic β-tetrapeptide, the bond angle differs from the inner angle of square, 90°, which will cause distortion of the cyclic skeleton from the planarity and/or of the pyranose ring from a stable chair conformation.

Peptide Synthesis. A key residue, 3-amino-2,6-anhydro-D-glycero-D-gulo-hepturonic acid hydrochloride **3**, was synthesized via 11 steps from D-glucosamine hydrochloride according to the literature.[9] Phenacyl ester (pac) group and *tert*-butoxycarbonyl (Boc) group in a protected sugar **4** synthesized from **3** were removed by zinc-catalyzed hydrogenolysis and TFA/anisole or 4 N HCl/1,4-dioxane treatment, respectively. When we attempted deprotection of pac group by Pd/C-catalyzed hydrogenolysis according to ref 9, an undesirable compound having a reduced phenacyl derivative was obtained as a major product. Therefore, we adopted the Zn/acetic acid (AcOH) hydrogenolysis method to avert this problem. Elongation reactions to the linear di-**5**, tri-**6**, and tetrapeptides **7** were carried out using *O*-(7-azobenzotriazol-1-yl)-1,1,3,3-tetramethyluronium hexafluorophosphate (HATU) as a coupling reagent. Cyclization reaction was carried out using 1-benzotriazolyloxytris(dimethylamino)phosphonium hexafluorophosphate (BOP), 1-hydroxy-7-azabenzotriazole (HOAT), and diisopropylethylamine (DIEA) in DMF (10 mM) (Scheme 1). The yields of the cyclization reactions of linear trimers and tetramers were relatively high, because the linear oligomers are reported to take helical structures.[10]

The trimer **1** was soluble in DMF, DMSO, TFE, 1,1,1,3,3,3-hexafluoro-2-propanol (HFIP), and TFA. On the other hand, the tetramer **2** was soluble in DMF, DMSO, HFIP, AcOH, and pyridine. Both compounds showed remarkable improvement of solubility by comparison with cyclic β-peptides in the previous reports.[26,28,30,41,43]

Spectroscopic Analysis and Assembly Formation. The trimer **1** was soluble in TFE, which made it possible to analyze assembly formation by CD spectroscopy. With the addition of ethanol to **1** in TFE, a dramatic change was observed in the region from 1/1 to 3/4 (TFE/ethanol v/v) (Figure 3). The excess addition of ethanol beyond 1/2 (TFE/ethanol v/v) decreased the intensity of CD signal due to the precipitation. The CD change is ascribed to molecular assembling of the cyclic peptide.

^{1}H NMR spectrum of **1** in DMSO-d_6 at room temperature showed three sharp peaks corresponding to H-4, H-6, and acetyl groups (CH_3CO−) in the glycamino acid residue and broad peaks of the rest protons. With elevating the temperature up to 80 °C, all signals became narrow and one signal appeared for each proton of the glycamino acid residue, indicating a C_3 symmetric conformation. There are two interpretations for the line-width narrowing; dissociation of the molecular assembly at the higher temperature or existence of multiple conformations with exchange rate comparable to the NMR time scale at room temperature. The former may be plausible, because the slightly hazy solution at room temperature became transparent at higher temperature. Further, the sharp signals are assigned to peripheral protons of the cyclic structure, which should be less influenced by intermolecular hydrogen bonds at the center of the cyclic structure in the case of assembly formation.

From the spectrum at 80 °C, the spin coupling constants between amide proton and H$^\beta$ and between H$^\alpha$ and H$^\beta$ in the glycamino acid residue were obtained as 9.04 and 10.5 Hz, respectively. With applying these values to the Karplus equation,[44,45] the dihedral angles of θ_1(H−N−C$^\beta$−H$^\beta$) and θ_2(H$^\alpha$−C$^\alpha$−C$^\beta$−H$^\beta$) were calculated to be 172° and approximately 180°, showing an anti relationship between the corresponding

Scheme 1. Synthetic Scheme of the Cyclic Trimer and Tetramer of Glycamino Acid[a]

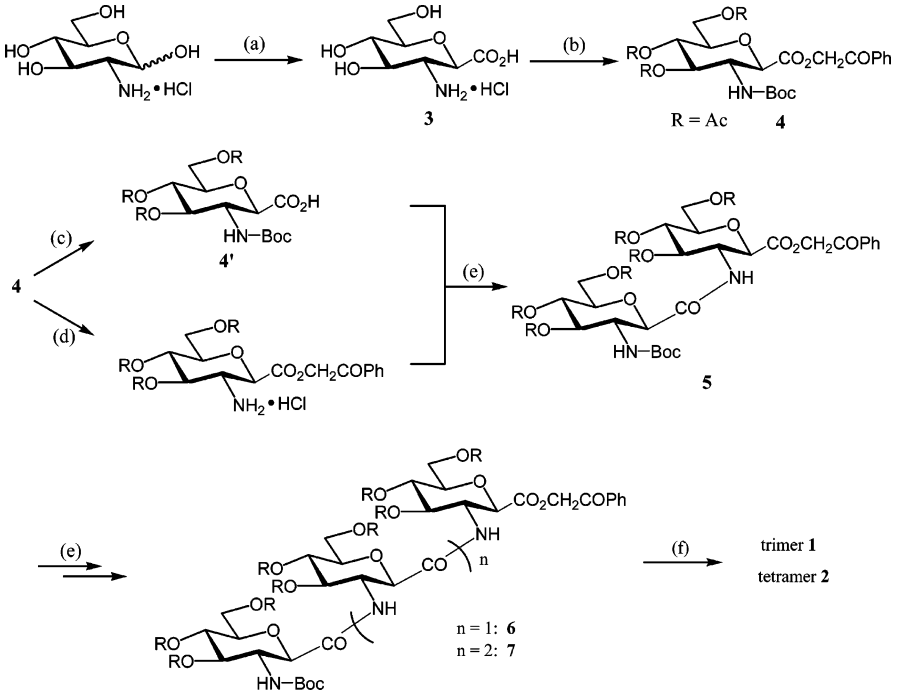

[a] Reagents and conditions: (a, b) 11 steps, in ref 9; (c) Zn/90% AcOH aq; (d) TFA/anisole; (e) elongation reaction using HATU and DIEA; (f) (i) Zn/90% AcOH aq, (ii) TFA/anisole, (iii) BOP, HOAT, DIEA/DMF.

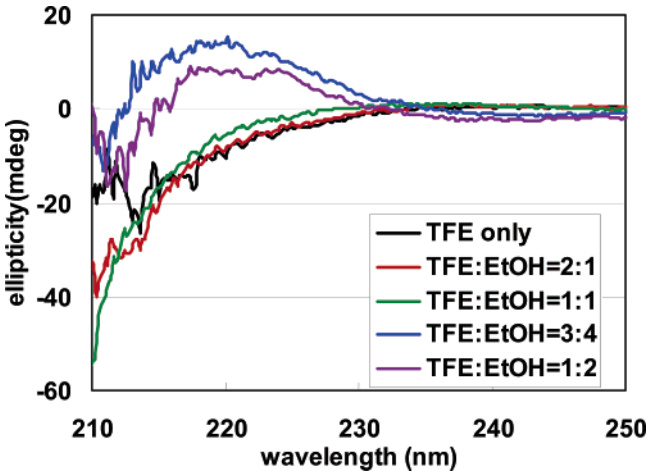

Figure 3. CD spectra demonstrating the assembly formation process of **1** in a mixed solution of 2,2,2-trifluoroethanol and ethanol.

H-atoms as the discussion in the peptide design section. ^{13}C NMR spectrum of **1** in DMSO-d_6 at 80 °C showed 13 carbon signals for one unit of GA(OAc), supporting again a C_3 symmetric conformation of **1** on an NMR time scale.

Assembly formation of the tetramer **2** could not be followed by CD spectroscopy, because **2** was not soluble in optically transparent solvents. However, ^1H NMR spectroscopy was applicable to analysis of assembly formation of **2**. ^1H NMR spectrum of the tetramer **2** in DMSO-d_6 at room temperature showed broad peaks, which became narrow at elevated temperatures, suggesting that **2** forms molecular assembly in DMSO-d_6 at room temperature as well as **1** and that the molecular assembly dissociates at the elevated temperatures. On the other hand, ^1H NMR spectrum of the tetramer **2** in pyridine-d_5 gave sharp peaks even at room temperature, suggesting that **2** should be soluble in pyridine without association. With the addition of acetonitrile, however, the solution became hazy probably due to assembly formation. Concentration dependence of NH chemical shift of **2** in pyridine-d_5/acetonitrile-d_3 (3/1 v/v) was examined (Figure 4). When the concentration of **2** exceeded over 0.25 mM, the chemical shift moved to a lower magnetic field with increasing the concentration. Intermolecular hydrogen bonds should be formed under these conditions probably to form molecular assembly.

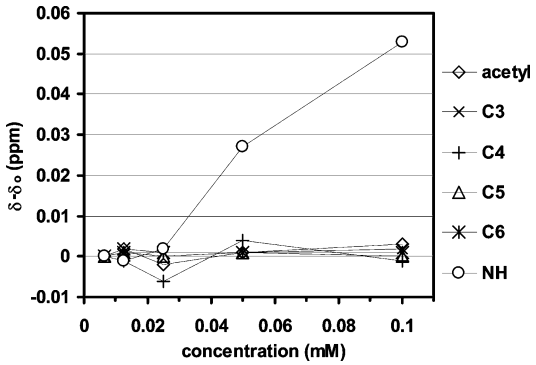

Figure 4. Concentration dependence of ^1H NMR chemical shifts of the cyclic tetramer **2** in a mixed solution of pyridine-d_5 and acetonitrile-d_3 (3/1 v/v).

In pyridine, the spin coupling constant between amide proton and H^β in the glycamino acid residue, and between H^α and H^β, were obtained as 8.0 and 11.5 Hz, respectively, and the dihedral angles $\theta_1(H-N-C^\beta-H^\beta)$ and $\theta_2(H^\alpha-C^\alpha-C^\beta-H^\beta)$, were calculated to be 159° and approximately 180°, respectively. The anti relationships of the corresponding H-atoms are also established in the tetramer **2**. The dihedral angle $\theta_1(H-N-C^\beta-H^\beta)$ of the cyclic tetramer **2** was 159°, which was smaller than that of 172° of the cyclic trimer **1**, suggesting that **2** is distorted with respect to the cyclic skeleton from the planarity and/or of the pyranose ring from a stable chair conformation as the discussion in the peptide design section. The ^{13}C NMR spectrum of **2** in pyridine-d_5 showed 13 carbon signals for one unit of GA(OAc) as well as the trimer **1**, indicating that **2** took a C_4 symmetric conformation.

FT-IR spectra of **1** and **2** in a solid state showed amide I absorption (mainly C═O stretching mode) at 1672 and 1690

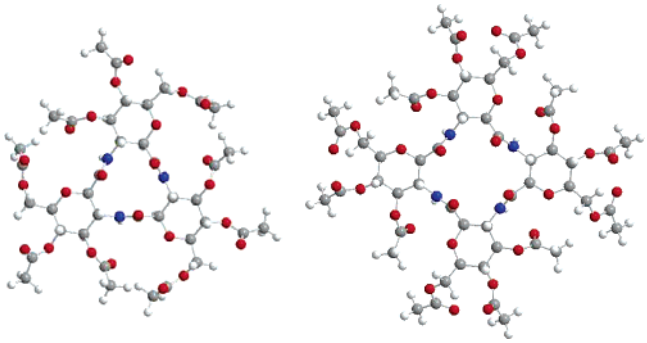

Figure 5. Energy-minimized structures of **1** (left) and **2** (right).

cm^{-1}, respectively, and amide II absorption (mainly N−H bending and C−N stretching mode) at 1570 and 1564 cm^{-1}, respectively, which may be assigned to absorptions of a parallel β-sheet structure. Both spectra of the two compounds showed a sharp N−H stretching absorptions (3298 cm^{-1} for **1** and 3294 cm^{-1} for **2**), suggesting that the hydrogen bonds should be formed homogeneously throughout the crystals of **1** and **2**.

Geometry Optimization. The conformations of **1** and **2** were studied further by computational geometry optimization. In the case of compound **1**, the optimized conformation having a C_3 symmetry axis was obtained as shown in Figure 5 (left). Compound **1** has a planar conformation with three *trans*-amide groups orienting perpendicularly to the ring plane. This ring conformation coincides with that of cyclic trimer of *trans*-2-aminocyclohexylcarboxylic acid (ACHC) in our previous work.[27] The dihedral angle θ_1(H−N−C$^{\beta}$−H$^{\beta}$) in this optimized conformation is 163°, which agrees well with the value calculated from the spin coupling constant between amide proton and H$^{\beta}$ in the glycamino acid residue. The optimized conformation of **2** is a C_4 symmetrical molecule with the dihedral angle θ_2(H−N−C$^{\beta}$−H$^{\beta}$) of 159°, which is also consistent with the result of NMR analysis (Figure 5, right). Seebach et al. have reported that cyclo(β-HAla)$_4$ took a C_2 symmetrical conformation,[26] while Ghadiri et al. have shown that cyclo(β-HTrp)$_4$ took a C_4 symmetrical conformation with a hole of ca. 2.7 Å in diameter, which is large enough to allow passage of small atoms. Compound **2** is similar to the latter in terms of the symmetric property.[41] However, the planarity of peptide bonds in **2** is slightly distorted in comparison with the regular tetragon previously reported for cyclic tetramers of β-amino acids without a pyranose ring.[41,42]

The calculated dipole moments were 12.4 D for **1** and 12.1 D for **2**. These large dipole moments are derived from amide groups with orientation perpendicular to the ring skeleton. The similar values of **1** and **2** despite the difference in the number of amide groups may be due to the different contribution of the dipole moment of acetyl groups between **1** and **2**. When the compound **2**, whose internal cavity is estimated to be ca. 2.0 Å, forms a tubular assembly through face-to-face molecular stacking via hydrogen bonds,[26,41] the nanotube with a large dipole moment will be a candidate of a conduit for vectorial ion or electron transfer.[36,46−50]

Microscopic Observation. The compound **1** formed rod-shaped crystals of several hundred micrometers in length and micrometer-order diameter, which are bundles of thinner needles from precise optical microscopic observation (Figure 6A). When the crystals of **1** were observed under the cross-nicol configuration with a sensitive tint plate inserted at 45°, the crystals showed yellow color (subtraction retardation) and blue color (addition retardation) in the cases of parallel relation between the long axis (optical axis) of the crystals and the z' axis of the tint plate and vertical relation between them, respectively (Figure 6B). The short axis of the crystals has a larger refractive index ($n_{\perp}$) than that of the long axis ($n_{\parallel}$) ($n_{\perp} > n_{\parallel}$), which is an opposite relation ($n_{\perp} < n_{\parallel}$) observed in the case of cyclo(ACHC)$_3$.[27] Although the amide groups, which are the major factor for the refractive index, should orient parallel to the long axis, acetyl groups at the side chains of **1** would make the refractive index of the short axis larger.

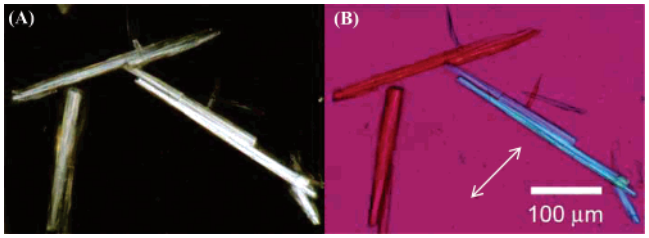

Figure 6. Optical microscopic observation without (A) and with a sensitive tint plate (B) in the cross-nicol configuration of **1** crystal. The double-headed arrow shows the orientation of the z' axis of a sensitive tint plate.

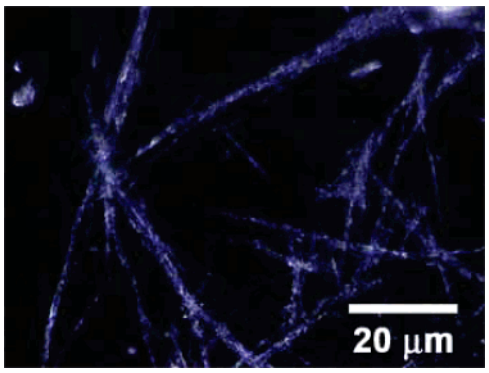

Figure 7. Dark field microscopic image of the molecular assembly of **2**.

The compound **2** did not grow large enough for optical microscopic observation. As discussed above, the molecular structure of **2** is distorted with respect to the cyclic skeleton from the planarity and/or of the pyranose ring from a stable chair conformation in comparison with that of **1**. Thus, **2** may not grow into large crystals. However, the crystals in a size of sub-micrometers were successfully observed by a dark field microscopy (Figure 7). Interestingly, the rod-shaped crystals took a partially helical arrangement. There are four hydrogen bonds formed between the stacking two cyclic peptides. A straight arrangement about N−H···O=C is most energetically stable, which may induce twist in the tubular structure. The twisting tubes will then assemble into bundles with helical sense. Similar speculation was proposed by Liu et al. for the case of cyclo[(−β^3-HGly)$_4$−] .[42]

The TEM image for the dispersion of fine crystals of compound **1** contains rod-shaped assemblies with high aspect ratio (Figure 8A). The morphology of the assemblies is relatively homogeneous especially on its width distribution (the most frequent width = ca. 35 nm). More than 50 microdiffraction patterns were obtained by using an incident electron beam perpendicular to the long axis. A typical diffraction pattern **1** is shown in Figure 9A. The molecular assembly was so fragile with an electron beam that the spots only on the meridian were observed. However, it is clearly shown that the unit cell has an axial spacing of ca. 4.8 Å, which is agreeable with the spacing between stacking two cyclic peptides in the tubular structure.

The TEM image of the tetramer **2** showed crystals with low aspect ratio (Figure 8B), but the helical arrangement was also

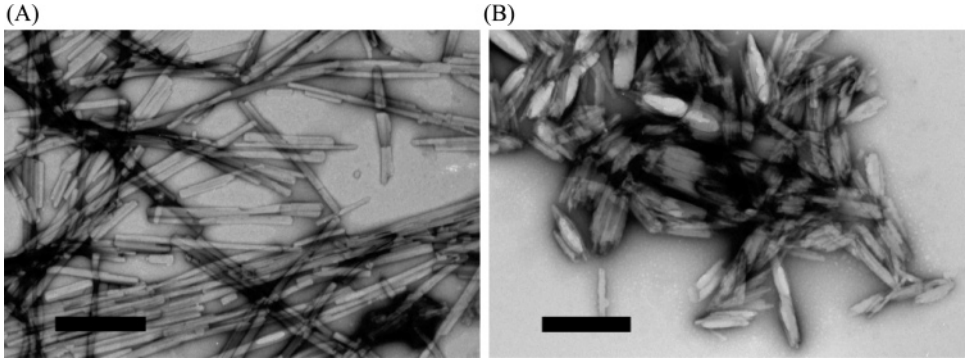

Figure 8. Negatively stained (2% uranyl acetate) TEM images of molecular assembly of **1** (A) and **2** (B). Bar = 500 nm.

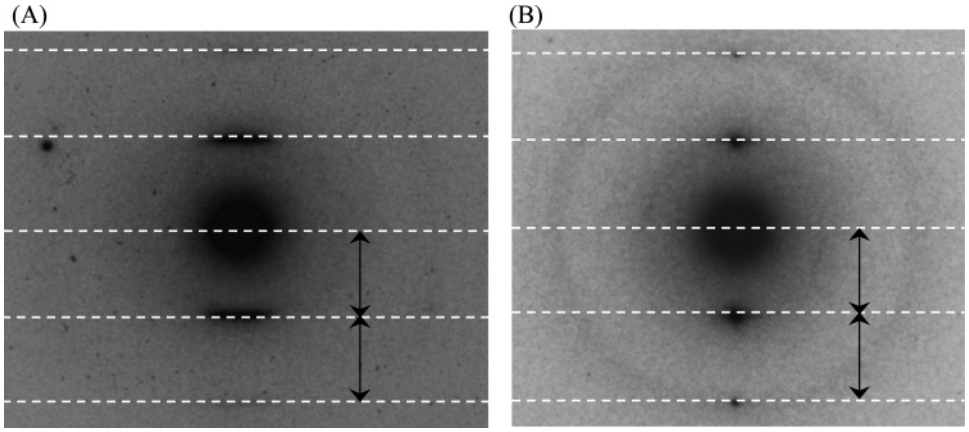

Figure 9. Electron diffraction patterns obtained with an incident electron beam perpendicular to the long axis of the molecular column of **1** (A) and **2** (B).

identified as that by the dark field microscopy. Layer spacing of the crystals was determined from electron diffraction pattern (Figure 9B) as spacing of ca. 4.8 Å, indicating that the tetramer should stack up into tubular structures.

The spacing distance between two cyclic peptides in the tubular structure was also estimated from the IR spectra of these crystals. The intermolecular distance between nitrogen atom and oxygen atom via a hydrogen bond in either crystal was evaluated as ca. 2.9 Å from the N−H stretching wavenumber according to the Krimm's method.[51] Since the distance between nitrogen atom and oxygen atom along the *z* axis is 1.9 Å by geometry optimization, the sum of the two distances is very close to the axial spacing evaluated from the diffraction analysis. Taken together, the two cyclic β-peptides in a solid state should form a "*nanotube*" via stacking of cyclic peptides, and the size of bundles can be controllable with adjusting solution composition and concentration due to the improved solubility.[27,28,30,31,52]

Conclusion

Novel cyclic tri- and tetra-β-peptides composed of glycamino acids were designed and synthesized. The solubility of these cyclic β-peptides were significantly improved from those reported previously to allow spectroscopic measurements in solution. TEM observation and electron diffraction analysis showed that both cyclic β-peptides stacked up into columnar structures via intermolecular hydrogen bonds between two cyclic peptides. Especially, the trimer formed homogeneous assembly with narrow width distribution. The cyclic glycopeptides will possess hydroxyl groups on the exterior of the tubular assembly after removal of the acetyl groups, which can be easily chemically modified and functionalized. This chemical modification is now under investigation.

Acknowledgment. The authors thank Dr. Y. Suhara at Kobe Pharmaceutical University for valuable advice in the synthesis. The authors also thank Professor Takao Itoh at Kyoto University for allowing us to use TEM and for technical advice. This work is financially supported by a Grant-in-Aid for Young Scientists B (16750098), Grant-in-Aid for Scientific Research B, and 21st century COE program (a United Approach to New Materials Science), from the Ministry of Education, Culture, Sports, Science, and Technology, Japan.

References and Notes

(1) Jensen, K. J.; Brask, J. *Biopolymers* **2005**, *80*, 747−761.
(2) Chakraborty, T. K.; Srinivasu, P.; Tapadar, S.; Mohan, B. K. *Glycoconjugate J.* **2005**, *22*, 83−93.
(3) Gruner, S. A. W.; Locardi, E.; Lohof, E.; Kessler, H. *Chem. Rev.* **2002**, *102*, 491−514.
(4) Chakraborty, T. K.; Ghosh, S.; Jayaprakash, S. *Curr. Med. Chem.* **2002**, *9*, 421−435.
(5) Chakraborty, T. K.; Jayaprakash, S.; Ghosh, S. *Comb. Chem. High Throughput Screening* **2002**, *5*, 373−387.
(6) Schweizer, F. *Angew. Chem., Int. Ed.* **2002**, *41*, 230−253.
(7) Peri, F.; Cipolla, L.; Forni, E.; La Ferla, B.; Nicotra, F. *Chemtracts: Org. Chem.* **2001**, *14*, 481−499.
(8) Schmidt, S.; Teich, L.; Khodja, M.; Sicker, D. *Lett. Org. Chem.* **2005**, *2*, 165−171.
(9) Suhara, Y.; Hildreth, J. E. K.; Ichikawa, Y. *Tetrahedron Lett.* **1996**, *37*, 1575−1578.
(10) Suhara, Y.; Yamaguchi, Y.; Collins, B.; Schnaar, R. L.; Yanagishita, M.; Hildreth, J. E. K.; Shimada, I.; Ichikawa, Y. *Bioorg. Med. Chem.* **2002**, *10*, 1999−2013.
(11) vonRoedern, E. G.; Lohof, E.; Hessler, G.; Hoffmann, M.; Kessler, H. *J. Am. Chem. Soc.* **1996**, *118*, 10156−10167.
(12) Denooy, A. E. J.; Besemer, A. C.; Vanbekkum, H. *Tetrahedron* **1995**, *51*, 8023−8032.
(13) Smith, M. D.; Long, D. D.; Marquess, D. G.; Claridge, T. D. W.; Fleet, G. W. J. *Chem. Commun.* **1998**, 2039−2040.
(14) Smith, M. D.; Fleet, G. W. J. *J. Pept. Sci.* **1999**, *5*, 425−441.

(15) Chakraborty, T. K.; Ghosh, S.; Jayaprakash, S.; Sharma, J.; Ravikanth, V.; Diwan, P. V.; Nagaraj, R.; Kunwar, A. C. *J. Org. Chem.* **2000**, *65*, 6441−6457.
(16) Poitout, L.; Lemerrer, Y.; Depezay, J. C. *Tetrahedron Lett.* **1995**, *36*, 6887−6890.
(17) Raunkjaer, M.; El Oualid, F.; van der Marel, G. A.; Overkleeft, H. S.; Overhand, M. *Org. Lett.* **2004**, *6*, 3167−3170.
(18) Menand, M.; Blais, J. C.; Hamon, L.; Valery, J. M.; Xie, J. *J. Org. Chem.* **2005**, *70*, 4423−4430.
(19) Stockle, M.; Voll, G.; Gunther, R.; Lohof, E.; Locardi, E.; Gruner, S.; Kessler, H. *Org. Lett.* **2002**, *4*, 2501−2504.
(20) van Well, R. M.; Marinelli, L.; Erkelens, K.; van der Marel, G. A.; Lavecchia, A.; Overkleeft, H. S.; van Boom, J. H.; Kessler, H.; Overhand, M. *Eur. J. Org. Chem.* **2003**, 2303−2313.
(21) van Well, R. M.; Overkleeft, H. S.; Overhand, M.; Carstenen, E. V.; van der Marel, G. A.; van Boom, J. H. *Tetrahedron Lett.* **2000**, *41*, 9331−9335.
(22) Gruner, S. A. W.; Truffault, V.; Voll, G.; Locardi, E.; Stockle, M.; Kessler, H. *Chem. Eur. J.* **2002**, *8*, 4366−4376.
(23) van Well, R. M.; Marinelli, L.; Altona, C.; Erkelens, K.; Siegal, G.; van Raaij, M.; Llamas-Saiz, A. L.; Kessler, H.; Novellino, E.; Lavecchia, A.; van Boom, J. H.; Overhand, M. *J. Am. Chem. Soc.* **2003**, *125*, 10822−10829.
(24) Chakraborty, T. K.; Srinivasu, P.; Bikshapathy, E.; Nagaraj, R.; Vairamani, M.; Kumar, S. K.; Kunwar, A. C. *J. Org. Chem.* **2003**, *68*, 6257−6263.
(25) Ghadiri, M. R.; Granja, J. R.; Milligan, R. A.; McRee, D. E.; Khazanovich, N. *Nature* **1993**, *366*, 324−327.
(26) Seebach, D.; Matthews, J. L.; Meden, A.; Wessels, T.; Baerlocher, C.; McCusker, L. B. *Helv. Chim. Acta* **1997**, *80*, 173−182.
(27) Fujimura, F.; Fukuda, M.; Sugiyama, J.; Morita, T.; Kimura, S. *Org. Biomol. Chem.* **2006**, *4*, 1896−1901.
(28) Gademann, K.; Seebach, D. *Helv. Chim. Acta* **1999**, *82*, 957−962.
(29) Clark, T. D.; Buriak, J. M.; Kobayashi, K.; Isler, M. P.; McRee, D. E.; Ghadiri, M. R. *J. Am. Chem. Soc.* **1998**, *120*, 8949−8962.
(30) Matthews, J. L.; Gademann, K.; Jaun, B.; Seebach, D. *J. Chem. Soc., Perkin Trans. 1* **1998**, 3331−3340.
(31) Matthews, J. L.; Overhand, M.; Kuhnle, F. N. M.; Ciceri, P. E.; Seebach, D. *Liebigs Ann.* **1997**, 1371−1379.
(32) Sugiyama, J.; Vuong, R.; Chanzy, H. *Macromolecules* **1991**, *24*, 4168−4175.
(33) Koyama, M.; Helbert, W.; Imai, T.; Sugiyama, J.; Henrissat, B. *Proc. Natl. Acad. Sci. U.S.A.* **1997**, *94*, 9091−9095.
(34) Cache Worksystems Pro Version 6.1.1; Fujitsu Limited: Tokyo, Japan, 2003.
(35) Frisch, M. J.; Trucks, G. W.; Schlegel, H. B.; Scuseria, G. E.; Robb, M. A.; Cheeseman, J. R.; Montgomery, J. A., Jr.; Vreven, T.; Kudin, K. N.; Burant, J. C.; Millam, J. M.; Iyengar, S. S.; Tomasi, J.; Barone, V.; Mennucci, B.; Cossi, M.; Scalmani, G.; Rega, N.; Petersson, G. A.; Nakatsuji, H.; Hada, M.; Ehara, M.; Toyota, K.; Fukuda, R.; Hasegawa, J.; Ishida, M.; Nakajima, T.; Honda, Y.; Kitao, O.; Nakai, H.; Klene, M.; Li, X.; Knox, J. E.; Hratchian, H. P.; Cross, J. B.; Bakken, V.; Adamo, C.; Jaramillo, J.; Gomperts, R.; Startmann, R. E.; Yazyev, O.; Austin, A. J.; Cammi, R.; Pomelli, C.; Ochterski, J.; Ayala, P. Y.; Morokuma, K.; Voth, G. A.; Salvador, P.; Dannenberg, J. J.; Zakrzewski, V. G.; Dapprich, S.; Daniels, A. D.; Strain, M. C.; Farkas, O.; Malick, D. K.; Rabuck, A. D.; Raghavachari, K.; Foresman, J. B.; Ortiz, J. V.; Cui, Q.; Baboul, A. G.; Clifford, S.; Cioslowski, J.; Stefanov, B. B.; Liu, G.; Liashenko, A.; Piskorz, P.; Komaromi, I.; Martin, R. L.; Fox, D. J.; Keith, T.; Al-Laham, M. A.; Peng, C. Y.; Nanayakkara, A.; Challacombe, M.; Gill, P. M. W.; Johnson, B. G.; Chen, W.; Wong, M. W.; Gonzalez, C.; Pople, J. A. *Gaussian 03* (Revision 02); Gaussian, Inc.: Wallingford, CT, 2004.
(36) Yasutomi, S.; Morita, T.; Imanishi, Y.; Kimura, S. *Science* **2004**, *304*, 1944−1947.
(37) Fukuda, M.; Sugiyama, J.; Morita, T.; Kimura, S. *Polym. J.* **2006**, *38*, 381−386.
(38) Yoshida, K.; Kawamura, S.; Morita, T.; Kimura, S. *J. Am. Chem. Soc.* **2006**, ASAP.
(39) Gauthier, D.; Baillargeon, P.; Drouin, M.; Dory, Y. L. *Angew. Chem., Int. Ed.* **2001**, *40*, 4635−4638.
(40) Locardi, E.; Stockle, M.; Gruner, S.; Kessler, H. *J. Am. Chem. Soc.* **2001**, *123*, 8189−8196.
(41) Clark, T. D.; Buehler, L. K.; Ghadiri, M. R. *J. Am. Chem. Soc.* **1998**, *120*, 651−656.
(42) Tan, H. W.; Qu, W. W.; Chen, G. J.; Liu, R. Z. *Chem. Phys. Lett.* **2003**, *369*, 556−562.
(43) Hoffmann, T.; Seebach, D. *Liebigs Ann.* **1996**, 1277−1282.
(44) Karplus, M. *J. Chem. Phys.* **1959**, *30*, 11−15.
(45) Fujimura, F.; Fukuda, M.; Sugiyama, J.; Morita, T.; Kimura, S. *Chem. Lett.* **2004**, *33*, 810−811.
(46) Morita, T.; Kimura, S.; Kobayashi, S.; Imanishi, Y. *J. Am. Chem. Soc.* **2000**, *122*, 2850−2859.
(47) Morita, T.; Kimura, S. *J. Am. Chem. Soc.* **2003**, *125*, 8732−8733.
(48) Yanagisawa, K.; Morita, T.; Kimura, S. *J. Am. Chem. Soc.* **2004**, *126*, 12780−12781.
(49) Yasutomi, S.; Morita, T.; Kimura, S. *J. Am. Chem. Soc.* **2005**, *127*, 14564−14565.
(50) Watanabe, J.; Morita, T.; Kimura, S. *J. Phys. Chem. B* **2005**, *109*, 14416−14425.
(51) Krimm, S.; Bandekar, J. In *Advances in Protein Chemistry*; Anifinsen, C. B., Edsall, J. T., Richards, F. M. Eds.; Academic Press: Orlando, FL, 1986; pp 181−364.
(52) Gademann, K.; Seebach, D. *Helv. Chim. Acta* **2001**, *84*, 2924−2937.

BM060415Y